This is a repository copy of *Climatic controls of decomposition drive the global biogeography of forest-tree symbioses*.

White Rose Research Online URL for this paper:
http://eprints.whiterose.ac.uk/146845/

Version: Accepted Version

Article:

Title: Climatic controls of decomposition drive the global biogeography of forest tree symbioses

Authors: Steidinger BS[1]*, Crowther TW[2]†*, Liang J†[3,4]*, Van Nuland ME[1], Werner GDA[5], Reich PB[6,7], Nabuurs G[8], de-Miguel S[9,10], Zhou M[3], Picard N[11], Herault B[12], Zhao X[4], Zhang C[4], Routh D[2] Abegg, Meinrad; Adou Yao, C. Yves; Alberti, Giorgio; Almeyda Zambrano, Angelica; Alvarez-Davila, Esteban; Alvarez-Loayza, Patricia; Alves, Luciana F.; Ammer, Christian; Antón-Fernández, Clara; Araujo-Murakami, Alejandro; Arroyo, Luzmila; Avitabile, Valerio; *Aymard, Gerardo; Baker, Timothy; Bałazy, Radomir; Banki, Olaf; Barroso, Jorcely; Bastian,* Meredith; Bastin, Jean-Francois; Birigazzi, Luca; Birnbaum, Philippe; Bitariho, Robert; Boeckx, Pascal; Bongers, Frans; Bouriaud, Olivier; Brancalion, Pedro H. S.; Brandl, Susanne; Brearley, Francis Q.; Brienen, Roel; Broadbent, Eben; Bruelheide, Helge; Bussotti, Filippo; Cazzolla Gatti, Roberto; Cesar, Ricardo; Cesljar, Goran; Chazdon, Robin; Chen, Han Y. H.; Chisholm, Chelsea; Cienciala, Emil; Clark, Connie J.; Clark, David; Colletta, Gabriel; Condit, Richard; Coomes, David; Cornejo Valverde, Fernando; Corral-Rivas, Jose J.; Crim, Philip; Cumming, Jonathan; Dayanandan, Selvadurai; de Gasper, André L.; Decuyper, Mathieu; Derroire, Géraldine; DeVries, Ben; Djordjevic, Ilija; Iêda, Amaral; Dourdain, Aurélie; Obiang, Nestor Laurier Engone; Enquist, Brian; Eyre, Teresa; Fandohan, Adandé Belarmain; Fayle, Tom M.; Feldpausch, Ted R.; Finér, Leena; Fischer, Markus; Fletcher, Christine; Fridman, Jonas; Frizzera, Lorenzo; Gamarra, Javier G. P.; Gianelle, Damiano; Glick, Henry B.; Harris, David; Hector, Andrew; Hemp, Andreas; Hengeveld, Geerten; Herbohn, John; Herold, Martin; Hillers, Annika; Honorio Coronado, Eurídice N.; Huber, Markus; Hui, Cang; Cho, Hyunkook; Ibanez, Thomas; Jung, Ilbin; Imai, Nobuo; Jagodzinski, Andrzej M.; Jaroszewicz, Bogdan; Johannsen, Vivian; Joly, Carlos A.; Jucker, Tommaso; Karminov, Viktor; Kartawinata, Kuswata; Kearsley, Elizabeth; Kenfack, David; Kennard, Deborah; Kepfer-Rojas, Sebastian; Keppel, Gunnar; Khan, Mohammed Latif; Killeen, Timothy; Kim, Hyun Seok; Kitayama, Kanehiro; Köhl, Michael; Korjus, Henn; Kraxner, Florian; Laarmann, Diana; Lang, Mait; Lewis, Simon; Lu, Huicui; Lukina, Natalia; Maitner, Brian; Malhi, Yadvinder; Marcon, Eric; Marimon, Beatriz Schwantes; Marimon-Junior, Ben Hur; Marshall, Andrew Robert; Martin, Emanuel; Martynenko, Olga; Meave, Jorge A.; Melo-Cruz, Omar; Mendoza, Casimiro; Merow, Cory; Monteagudo Mendoza, Abel; Moreno, Vanessa; Mukul, Sharif A.; Mundhenk, Philip; Nava-Miranda, Maria G.; Neill, David; Neldner, Victor; Nevenic, Radovan; Ngugi, Michael; Niklaus, Pascal; Oleksyn, Jacek; Ontikov, Petr; Ortiz-Malavasi, Edgar; Pan, Yude; Paquette, Alain; Parada-Gutierrez, Alexander; Parfenova, Elena; Park, Minjee; Parren, Marc; Parthasarathy, Narayanaswamy; Peri, Pablo L.; Pfautsch, Sebastian; Phillips, Oliver; Piedade, Maria Teresa; Piotto, Daniel; Pitman, Nigel C. A.; Polo, Irina; Poorter, Lourens; Poulsen, Axel Dalberg; Poulsen, John R.; Pretzsch, Hans; Ramirez Arevalo, Freddy; Restrepo-Correa, Zorayda; Rodeghiero, Mirco; Rolim, Samir; Roopsind, Anand; Rovero, Francesco; Rutishauser, Ervan; Saikia, Purabi; Saner, Philippe; Schall, Peter; Schelhaas, Mart-Jan; Schepaschenko, Dmitry; Scherer-Lorenzen, Michael; Schmid, Bernhard; Schöngart, Jochen; Searle, Eric; Seben, Vladimír; Serra-Diaz, Josep M.; Salas-Eljatib, Christian; Sheil, Douglas; Shvidenko, Anatoly; Silva-Espejo, Javier; Silveira, Marcos; Singh, James; Sist, Plinio; Slik, Ferry; Sonké, Bonaventure; Souza, Alexandre F.; *Stereńczak, Krzysztof; Svenning, Jens*-Christian; Svoboda, Miroslav; Targhetta, Natalia; Tchebakova, Nadja; Steege, Hans ter; Thomas, Raquel; Tikhonova, Elena; Umunay, Peter; Usoltsev, Vladimir; Valladares, Fernando; van der Plas, Fons; Van Do, Tran; Vasquez Martinez, Rodolfo; Verbeeck, Hans; Viana, Helder; Vieira,

47 Simone; von Gadow, Klaus; Wang, Hua-Feng; Watson, James; Westerlund, Bertil; Wiser,
48 Susan; Wittmann, Florian; Wortel, Verginia; Zagt, Roderick; Zawila-Niedzwiecki, Tomasz; Zhu,
49 Zhi-Xin; Zo-Bi, Irie Casimir and Peay KG[1]†

50

51 **Affiliations:**
52 [1] Department of Biology, Stanford University, Stanford CA USA
53 [2] Department of Environmental Systems Science, ETH Zürich, Zürich, Switzerland
54 [3] Department of Forestry and Natural Resources, Purdue University, West Lafayette, IN, USA
55 [4] Research Center of Forest Management Engineering of State Forestry Administration, Beijing
56 Forestry University, Beijing, China
57 [5] Department of Zoology, University of Oxford, Oxford UK
58 [6] Department of Forest Resources, University of Minnesota
59 [7] Hawkesbury Institute for the Environment, Western Sydney University
60 [8] Wageningen University and Research
61 [9] Departament de Producció Vegetal i Ciència Forestal, Universitat de Lleida-Agrotecnio Center
62 [10] Forest Science and Technology Centre of Catalonia (CTFC)
63 [11] Food and Agriculture Organization of the United Nations
64 [12] Cirad, INP-HB, Univ Montpellier, UPR Forêts et Sociétés

65

66 *These authors contributed equally to this work and share the first-author
67 †Corresponding authors: Email kpeay@stanford.edu; albeca.liang@gmail.com;
68 tom.crowther@usys.ethz.ch

69

70   **The identity of the dominant microbial symbionts in a forest determines the ability**

71 **of trees to access limiting nutrients from atmospheric or soil pools[1,2], sequester**

72 **carbon[3,4] and withstand the impacts of climate change[1-7]. Characterizing the global**

73 **distribution of symbioses, and identifying the factors that control it, are thus integral to**

74 **understanding present and future forest ecosystem functioning. Here we generate the first**

75 **spatially explicit map of forest symbiotic status using a global database of 1.2 million forest**

76 **inventory plots with over 28,000 tree species. Our analyses indicate that climatic variables,**

77 **and in particular climatically-controlled variation in decomposition rate, are the primary**

78 **drivers of the global distribution of major symbioses. We estimate that ectomycorrhizal**

79 **(EM) trees, which represent only 2% of all plant species[8], constitute approximately 60% of**

80 **tree stems on Earth. EM symbiosis dominates forests where seasonally cold and dry**

climates inhibit decomposition, and are the predominant symbiosis at high latitudes and elevation. In contrast, arbuscular mycorrhizal (AM) trees dominate aseasonally warm tropical forests and occur with EM trees in temperate biomes where seasonally warm-and-wet climates enhance decomposition. Continental transitions between AM and EM dominated forests occur relatively abruptly along climate driven decomposition gradients, which is likely caused by positive plant-microbe feedbacks. Symbiotic N-fixers, which are insensitive to climatic controls on decomposition compared with mycorrhizal fungi, are most abundant in arid biomes with alkaline soils and high maximum temperatures. The climatically driven global symbiosis gradient we document represents the first spatially-explicit, quantitative understanding of microbial symbioses at the global scale and demonstrates the critical role of microbial mutualisms in shaping the distribution of plant species.

Microbial symbionts strongly influence the functioning of forest ecosystems. They exploit inorganic, organic[2] and/or atmospheric forms of nutrients that enable plant growth[1], determine how trees respond to elevated CO_2[6], regulate the respiratory activity of soil microbes[3,9], and affect plant species diversity by altering the strength of conspecific negative density dependence[10]. Despite growing recognition of the importance of root symbioses for forest functioning[1,6,11] and the potential to integrate symbiotic status into Earth system models that predict functional changes to the terrestrial biosphere[11,12], we lack spatially-explicit, quantitative maps of the different root symbioses at the global scale. Generating these quantitative maps of tree symbiotic states would link the biogeography of functional traits of belowground microbial symbionts with their 1.5 trillion host trees[13], spread across Earth's forests, woodlands, and savannas.

104   The dominant guilds of tree root symbionts, arbuscular mycorrhizal (AM) fungi,

105   ectomycorrhizal (EM) fungi, ericoid mycorrhizal (ErM) fungi, and nitrogen (N)-fixing bacteria

106   (N-fixer) are all based on the exchange of plant photosynthate for limiting macronutrients. The

107   AM symbiosis is the oldest of the four, having evolved nearly 500 million years ago, with EM,

108   ErM and N-fixer plant taxa having evolved multiple times from an AM basal state. Plants that

109   form the AM symbiosis are markedly more diverse than the other symbiotic groups, comprising

110   nearly 80% of all terrestrial plant species, and principally rely on AM fungi for enhancing

111   mineral phosphorus (P) uptake[14]. EM fungi evolved more recently from saprotrophic ancestors,

112   and as a result may be better than AM fungi at competing with free living soil microbes for

113   resources[3]. As such, some EM fungal lineages are more capable of mobilizing organic sources of

114   soil nutrients (particularly nitrogen) compared with AM fungi[15,16]. Association with EM fungi,

115   but not AM fungi, has been shown to allow trees to accelerate photosynthesis in response to

116   increased atmospheric CO_2 when soil nitrogen (N) is limiting[6] and to inhibit soil respiration by

117   decomposer microbes[3,9] (but see [17]). Because increased plant photosynthesis and decreased soil

118   respiration both reduce atmospheric CO_2 concentrations, the EM symbiosis is associated with

119   buffering the Earth's climate against anthropogenic changes.

120   In contrast to mycorrhizal fungi, which extract nutrients from the soil, symbiotic N-fixers

121   (Rhizobia and Actinobacteria) convert atmospheric N_2 to plant-usable forms. Symbiotic N-fixers

122   are responsible for a large fraction of biological soil-N inputs, which can increase N-availability

123   in forests where they are locally abundant[18]. Both N-fixing bacteria and EM fungi often demand

124   more plant photosynthate than does the AM symbiosis[14,19,20]. Because tree growth and

125   reproduction are limited by access to inorganic, organic and atmospheric sources of N, the

126   distribution of these root symbioses is likely to reflect both environmental conditions that

127   maximize the cost-benefit ratio of symbiotic exchange as well as physiological constraints on

128   different symbionts.

129   In one of the earliest efforts to understand the functional biogeography of plant root

130   symbioses, Sir David Read[21] categorically classified biomes by their perceived dominant

131   mycorrhizal type and hypothesized that seasonal climates favor hosts associating with EM fungi

132   due to their ability to compete directly for organic N. By contrast, it has been proposed that

133   sensitivity to low temperatures has prevented N-fixers from dominating outside the tropics,

134   despite the potential for N-fixation to alleviate N-limitation in boreal forests[20,22]. However,

135   global scale tests of these proposed biogeographic patterns and their proposed climate drivers are

136   lacking or inconclusive[23-25] and we have no understanding of the regional variations in this

137   proposed latitudinal trend. To address this research gap, we compiled the first global ground-

138   sourced survey database to reveal numerical abundances of each symbiosis across the global

139   forested biomes, rather than incidence (presence or absence, e.g.,[23-25]), which is essential for

140   identifying the shapes and potential mechanisms underlying transitions in forest symbiotic state

141   along climatic gradients[26,27].

142   We determined the abundance of tree symbioses using GFBi, an extension from the plot-

143   based Global Forest Biodiversity (GFB[28]) database, which contains over 1.2 million forest

144   inventory plots of individual-based measurement records from which we derive abundance

145   information for entire tree communities (Figure 1).

146
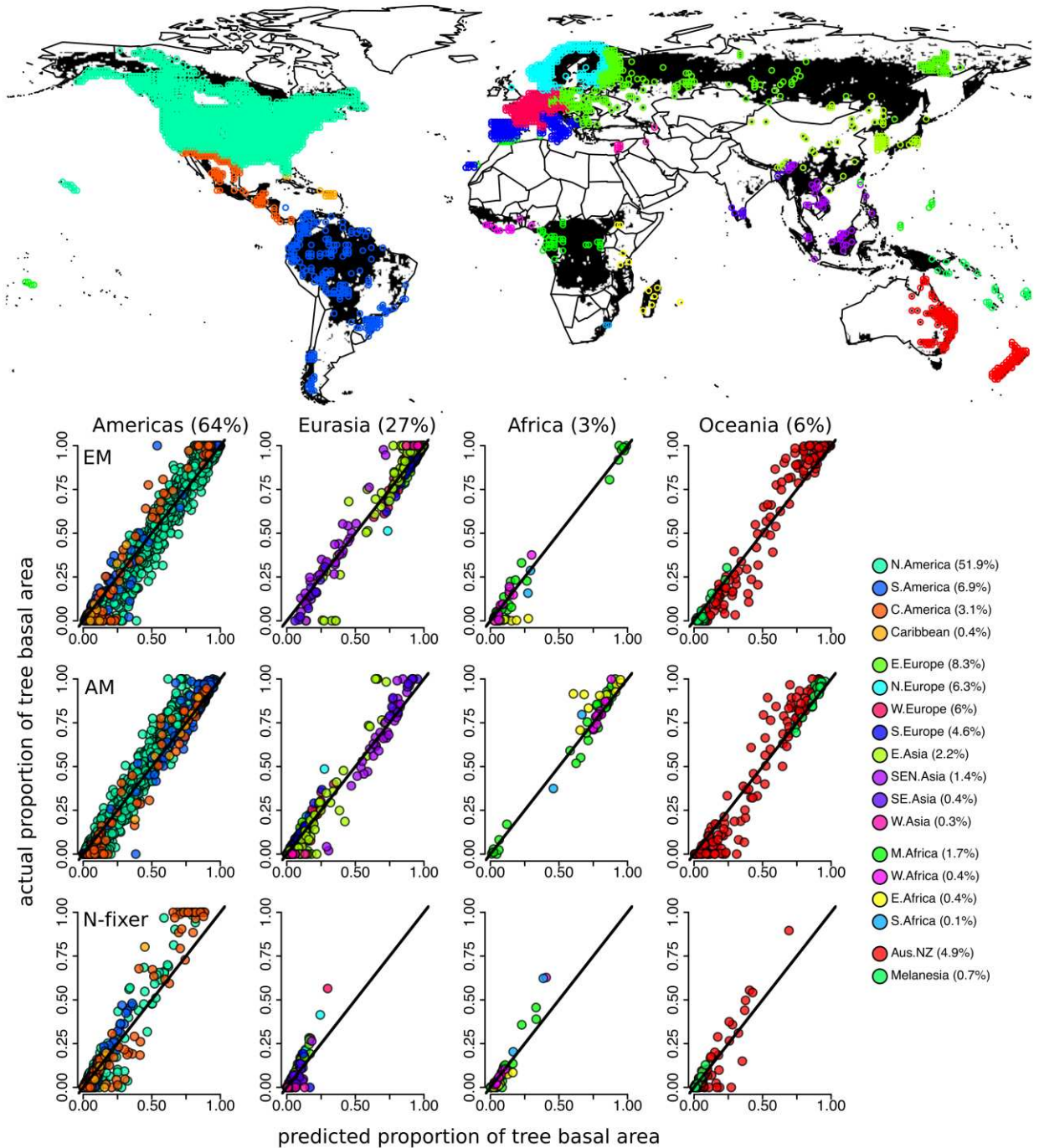
Figure 1. A map of 1 by 1 degree grid cells where we analyzed the proportion of tree stems and basal area for different symbiotic guilds (above). Circles show the location of training data, colored by geographic origin, while black squares show the extent of model projections. Panels below the map show actual vs. predicted proportion of basal area for ectomycorrhizal (EM), arbuscular mycorrhizal (AM), and N-fixer trees by continent and subregion, and demonstrate globally consistent model performance.

153 Using published literature on the evolutionary histories of mycorrhizal and N-fixer

154 symbioses[8,25,29-33], we assigned plant species from the GFBi to one of 5 symbiotic guilds: AM,

155 EM, ErM, N-fixer, and non- or weakly-mycorrhizal (NM). Most plants with symbioses derived

156 from the AM state retain the genetic potential to associate with AM fungi[14]. Thus, consistent

157 with other studies in this field[29], we assigned tree species to the AM-exclusive guild if they were

158 not EM, ericoid mycorrhizal, non-mycorrhizal, or N-fixers. While there is some uncertainty in

159 such assignments, direct investigation of mycorrhizal status when done supports this

160 assumption[34]. Because individual measurements of mycorrhizal colonization are not possible at

161 this scale, our models represent potential symbiotic associations.

162 To identify the key factors structuring symbiotic distributions we assembled 70 global

163 predictor layers: 19 climatic (annual, monthly, and quarterly temperature and precipitation

164 variables), 14 soil chemical (total soil N density, microbial N, C:N ratios and soil P fractions,

165 pH, cation exchange capacity), 5 soil physical (soil texture and bulk density), 26 vegetative

166 indices (leaf area index, total stem density, enhanced vegetation index means and variances), and

167 5 topographic variables (elevation, hillshade) (Table S7). Because decomposition is the dominant

168 process by which soil nutrients become available to plants, we generated 5 additional layers that

169 estimate the climatic control of decomposition. We parameterized decomposition coefficients

170 according to the Yasso07 model[35,36] using the following equation:

171

$$k = \mathrm{Exp}(0.095 T_i - 0.00014\ T_i^2)\ (1 - \mathrm{Exp}[\ -1.21\ P_i]), \qquad\qquad (1)$$

172 where P_i and T_i are precipitation and mean temperature, either quarterly or annually, and the

173 constants 0.0095 $(=\beta_1)$ $_=$0.00014 $(=\beta_2)$, and -1.21 $(=\gamma)$ are parameters fit using a previous global

174 study of leaf litter mass-loss[36]. Although local decomposition rates can vary significantly based

175 on litter quality or microbial community composition[37], climate is the primary control at the

176   global scale[36]. Decomposition coefficients describe how fast different chemical pools of leaf

177   litter lose mass over time relative to a parameter, $α$, that accounts for leaf-chemistry.

178   Decomposition coefficients (k) with values of 0.5 and 2 indicate a halving and doubling of

179   decomposition rates relative to $α$, respectively (Supplemental Materials).

180   Given the large set of possible environmental predictors, we used the random forest

181   machine-learning algorithm to identify the best predictors of global symbiosis distributions. The

182   random forest algorithm averages multiple regression trees, each of which uses a random subset

183   of all the model variables to predict a response. These regression trees identify optimal values

184   along a predictor-gradient to "split" the model response into different nodes (e.g., predictions

185   could be "split" into nodes of 50 or 75% of EM basal area depending on whether mean annual

186   temperature is > or < 20°C). We ranked the importance of each variable according to inc node

187   purity, which measures the decrease in model error that occurs whenever the response is split on

188   that variable (Figure 2ABC). We first determined the influence and relationship of all 75

189   predictor layers on forest symbiotic state and then optimized our models using a stepwise

190   reduction in variables, from least- to most-important. Soil chemical, vegetative, and topographic

191   variables were the first to be eliminated from our models in this way. In a subsequent model that

192   included only layers of climate, decomposition, and certain soil physical and chemical

193   information, we found that the 4 most important variables accounted for >85% of the explained

194   variability. We plot the partial-fits of these four variables for each symbiotic guild (Figure

195   2ABC).
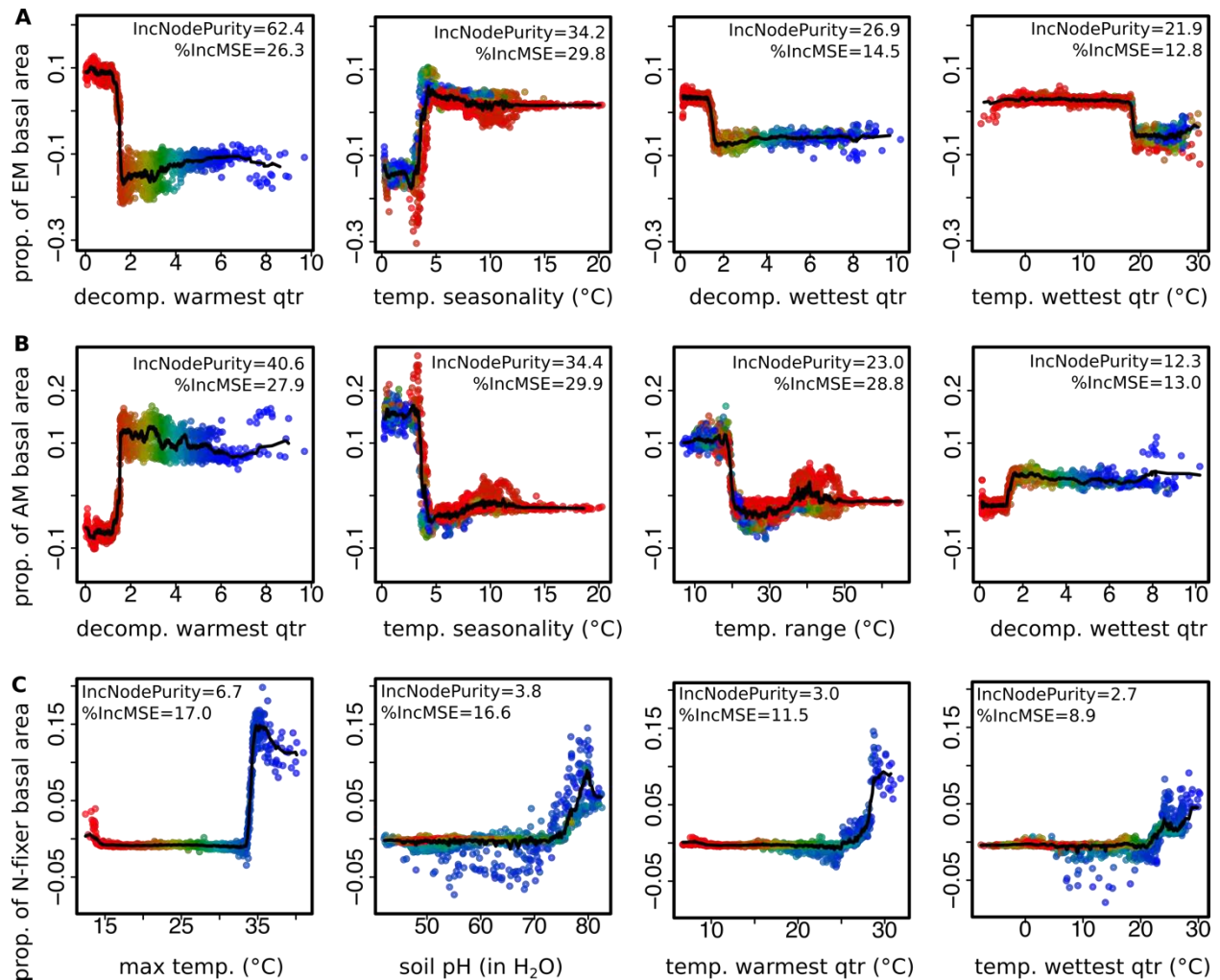
Figure 2. Partial plots of residual variation explained by the four most important predictors of the proportion of tree basal area belonging to the (A) ectomycorrhizal (EM), (B) arbuscular mycorrhizal (AM), and (C) N-fixer symbiotic guilds. Variables are listed in declining importance from left to right, as determined by inc node purity, with points colored with a red-green-blue gradient according to their position on the x-axis of the most important variable (left-most panels for each guild), allowing cross visualization between predictors. Each panel lists two measures of variable importance, inc node purity (used for sorting) and %IncMSE (see Supplemental Information for description). Decomposition rates in (A) and (B) are in units of leaf litter mass loss per quarter. The abundance of each symbiont type transitions sharply along climatic gradients, suggesting that sites near the threshold are particularly vulnerable to switching their dominant symbiont guild with climate changes.

The three most numerically abundant tree symbiotic guilds each have reliable environmental signatures, with the four most important predictors accounting for 81, 79, and 52% of the total variability in EM, AM, and N-fixer relative basal area, respectively. Models for

9

212   ErM and NM lack strong predictive power given the relative rarity of these symbiotic states

213   amongst trees, although the raw data do identify some local abundance hotspots for ErM (Figure

214   S1).   As a result, we focus the remainder of results and discussion on the three major tree

215   symbiotic states (EM, AM, N-fixer). Despite the fact that data from N. and S. America constitute

216   65% of the training data (at the 1 by 1 degree grid scale), our models accurately predict the

217   proportional abundances of the three major symbioses across all major geographic regions

218   (Figure 1). The high performance of our models, which is robust to both K-fold cross-validation

219   and rarefying samples so that all continents are represented with equal depth (Figures S10-12),

220   suggest that regional variations in climate (including indirect effects on decomposition) and soil

221   pH (for N-fixers) are the primary factors influencing the relative dominance of each guild at the

222   global scale (geographic origin only explained ~2-5% of the variability in residual relative

223   abundance) (Figure 1BCD, Table S8).

224   Random forest models should not be projected across predictor gradients that fall outside

225   the ranges of their training data (e.g., grid cells with higher mean annual temperatures than the

226   maximum used to fit the models). To prevent the over-projecting of our models over pixels

227   where we lacked training data, we subset a global grid of predictor layers depending on whether

228   (1) the grid cell fell within the top 60% of land surface with respect to tree stem density[13] and

229   either (2) fell within the univariate distribution of all the predictor layers from our training data

230   and/or (3) fell within an 8-dimensional hypervolume defined by the unique set of the 4-best

231   predictors of the relative abundance of each guild (Figure 2, Supplemental Materials). We then

232   projected our models across only those grid cells that met these criteria, which constitutes 46%

233   of the global land surface and 88% of global tree stems (Figure 1; Figure S16). While model

234   validation indicates that our projections are robust, additional ground truthing of predictions to

235 identify any discrepancies would be incredibly valuable. If such discrepancies exist they can

236 help fine tune climate-symbiosis models, or identify areas where climate might favors invasion

237 by symbioses that have not yet evolved or dispersed to a particular biogeographic region.

238   In contrast to a recent global analysis of root traits, which concluded that plant evolution

239 has favored reduced dependence on mycorrhizal fungi[38], we find that trees associating with the

240 relatively more C-demanding and recently-derived EM fungi[14,19] represent the dominant tree-

241 symbiosis. By taking the average proportion of EM trees, weighted by spatially-explicit global

242 predictions for tree stem density[13], we estimate that approximately 60% of trees on earth are EM,

243 despite the fact that only 2% of plant species associate with EM fungi (vs. 80% associating with

244 AM fungi)[8,29]. Outside of the tropics, the estimate for EM relative abundance increases to

245 approximately 80% of trees.

246   Turnover among the major symbiotic guilds results in a tri-modal latitudinal abundance

247 gradient, with the proportion of EM trees increasing (and AM trees decreasing) with distance

248 from the equator, while N-fixing trees reach peak abundance in the arid zone around 30 degrees

249 (Figure 3A, Figure 4). These trends are driven by abrupt transitional regions along continental

250 climatic gradients (Figure 2), which skew the distribution of symbioses among biomes (Figure

251 3A) and drive strong patterns across geographic and topographic features that influence climate.

252 For example, moving north or south from the equator, the first transitional zone separates warm

253 (aseasonal), AM-dominated, tropical broadleaf forests (>75% median basal area, vs. 8% for EM

254 trees) from the rest of the EM-dominated world forest system (Figure 2AB; Figure 3A). It

255 stretches longitudinally across 25 degrees N and S, just beyond the dry tropical broadleaf forests

256 (with 25% EM tree basal area; Figure 3A), where average monthly temperature variation reaches

257 3-5°C (Figure 2AB).

Figure 3. (A) The median proportion of tree basal area per biome (arranged in order of increasing mean temperature of the warmest quarter) for ectomycorrhizal (EM), arbuscular mycorrhizal (AM), and N-fixer symbiotic guilds. EM trees dominate all extra-tropical biomes. (B) The dependency of decomposition coefficients (k, solid and dotted lines) on temperature and precipitation during the warmest quarter with respect to predicted dominance of mycorrhizal symbiosis. AM forests transition to EM forests abruptly in the region between k=1 and 2, which is consistent with positive feedback between climatic and biological controls of decomposition.

258   Moving further N or S, the second transitional climate zone separates regions where

259   decomposition coefficients during the warmest quarter of the year are less than 2 (see Figure 3B

260   for the associated temperature and precipitation ranges). In N. America and China, this transition

261   zone spans longitudinally around 50 degrees N, separating the mixed AM / EM temperate forests

262   from their neighboring EM dominated boreal forests (75 vs 100% EM tree basal area,

263   respectively; Figure 3A). This transitional decomposition zone bypasses W. Europe, which has

264   temperature seasonality > 5°C, but lacks sufficiently wet summers to accelerate decomposition

265   coefficients beyond values associated with mixed AM/EM forests. The latitudinal transitions in

266   symbiotic state observed among biomes are mirrored by within-biome transitions along elevation

267 gradients. For example, in tropical Mexico, warm and wet quarter decomposition coefficients <

268 2 occur along the slopes of the Sierra Madre, where mixed AM-exclusive and N-fixer woodlands

269 in arid climates transition to EM dominated tropical coniferous forests (75% basal area, Figure

270 3A, Figure 4ABC, Figure S17-19). The southern hemisphere, which lacks the landmass to

271 support extensive boreal forests, experiences a similar latitudinal transition in decomposition

272 rates along the ecotone separating its tropical and temperate biomes, around 28 degrees S.

273   The abrupt transitions that we detected between forest symbiotic states along

274 environmental gradients suggest that positive feedbacks may exist between climatic and

275 biological controls of decomposition[11,36]. In contrast to AM fungi, some EM fungi can use

276 oxidative enzymes to mineralize organic nutrients from leaf litter, converting nutrients to plant-

277 usable forms before transferring them to their host trees[2,5]. Relative to AM trees, the leaf litter of

278 EM trees is also chemically more resistant to decomposition, with higher C:N ratios and higher

279 concentrations of decomposition-inhibiting secondary compounds[11]. Thus, EM leaf litter can

280 exacerbate climatic barriers to decomposition, promoting conditions where EM fungi have

281 superior nutrient-acquiring abilities to AM-fungi[5,11]. Such positive-feedbacks are known to cause

282 abrupt ecosystem transitions along smooth environmental gradients between woodlands and

283 grasses: trees suppress fires, which promotes seedling recruitment, while grass fuels fires, which

284 kill tree seedlings[39]. Our study provides the first evidence that rapid transitions in tree

285 community structure along climate gradients could also be governed by positive-feedbacks

286 between symbiotic guilds and nutrient cycling; although other types of interactions, such as

287 environmentally sensitive competition hierarchies among symbiotic guilds, could also lead to

288 abrupt transitions without specifically invoking feedback effects. In either case, the existence of

289 abrupt transitions suggests that trees and associated microbial symbionts in transitional regions

290   along decomposition gradients should be susceptible to drastic turnover in symbiotic state with

291   future environmental changes[40].

292   To illustrate the sensitivity of global patterns of tree symbiosis to climate change, we use

293   the climate relationships we developed for current climate to project potential changes due to

294   climate change. Relative to our global predictions using the most recent climate data, model

295   predictions using the projected climates for 2070 suggest the abundance of EM trees will decline

296   by as much as 10% (using a relative concentration pathway of 8.5 W/m^2; Figure S25). Due to

297   their position along decomposition gradients relative to the abrupt shift from EM to AM forests

298   (Figure 2AB), our models predict the largest declines in EM abundance will occur along the

299   boreal-temperate ecotone, although declines in species abundances can lag decades, or even

300   centuries or millennia, behind associated climatic changes[41]. The predicted decline in EM trees

301   corroborates the results of common garden transfer and simulated warming experiments, which

302   demonstrate that some important EM hosts will decline at the boreal-temperate ecotone in altered

303   climates[42-44]. Because of the low tree diversity in boreal forests, tree species loss around

304   transition zones may have major consequences for forest related economic activity[45].

305

306

307
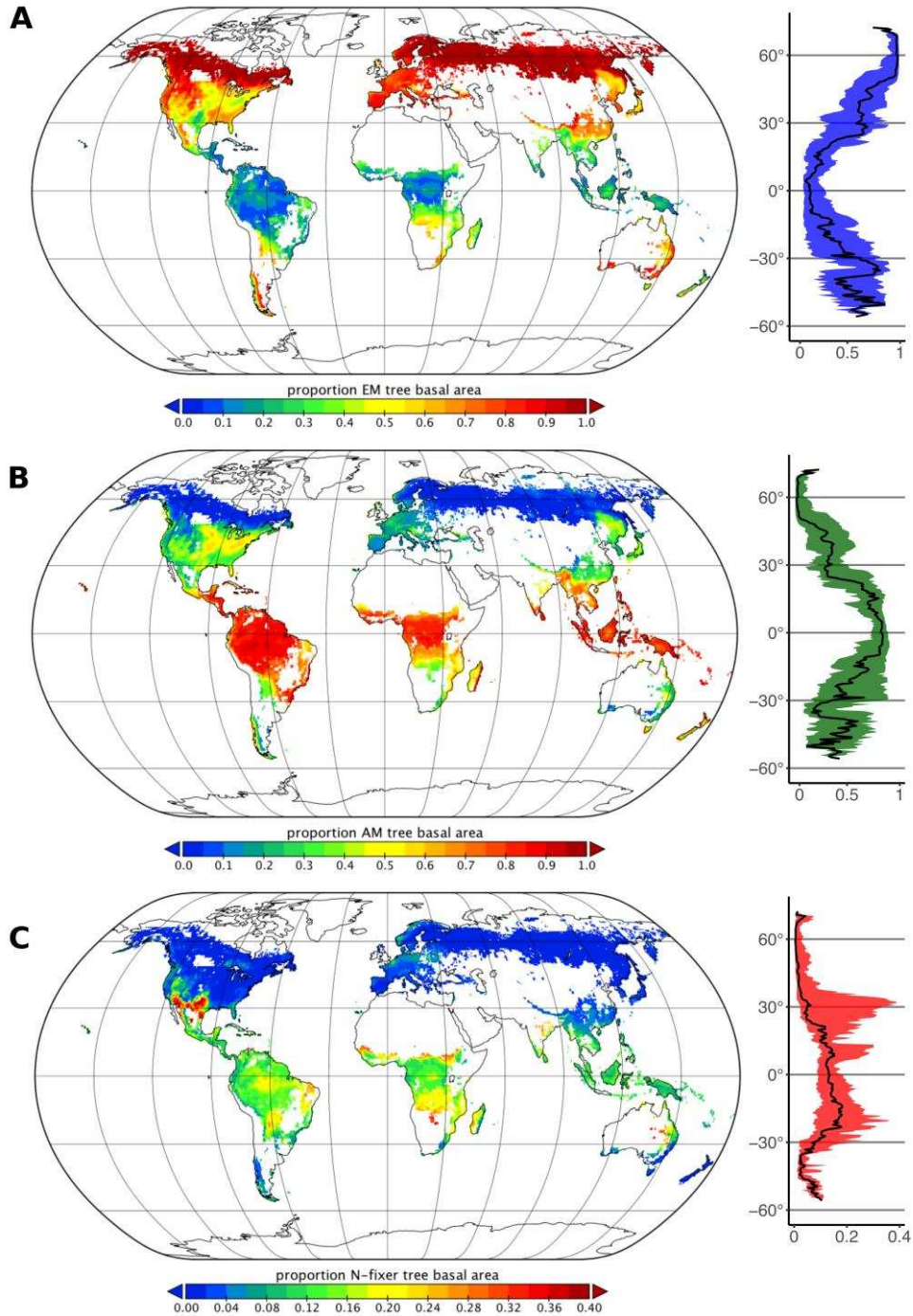
Figure 4. Predicted global maps (left) and latitudinal gradients (right, with solid line indicating the median and colored ribbon spanning the range from the 5% and 95% quantiles) of the proportion of tree basal area for (A) ectomycorrhizal (EM), (B) arbuscular mycorrhizal (AM), and (C) N-fixer symbiotic guilds.

308
309
310
311
312

313   The change in dominant nutrient exchange symbioses along climate gradients highlights

314   the interconnection between atmospheric and soil compartments of the biosphere. The transition

315   from AM to EM dominance corresponds with a shift from P to N limitation of plant growth with

316   increasing latitude[46-48]. Including published global projections of total soil N or P, microbial N,

317   or soil P fractions (labile, occluded, organic, and apatite) did not increase the amount of variation

318   explained by the model or alter the variables identified as most important, and thus were dropped

319   from our analysis. However, this does not necessarily mean that soil nutrient availability is

320   unimportant at the global scale, as the best-available global data likely do not adequately

321   represent local nutrient availability[49,50]. Rather, our finding that climatic controls of

322   decomposition best predict the dominant mycorrhizal associations mechanistically links

323   symbiont physiology with climatic controls of soil nutrient release from leaf litter. These

324   findings are consistent with Read's hypothesis[21] that slow decomposition at high latitudes favors

325   EM fungi due to their increased capacity to liberate organic nutrients[2]. Thus, while more

326   experiments are necessary to understand the specific mechanism by which nutrient competition

327   favors dominance of AM or EM symbioses[26], we propose that the latitudinal and elevational

328   transitions from AM to EM dominated forests be called Read's Rule.

329   While our analyses focus on prediction at large spatial scales appropriate to the available

330   data, our findings with respect to Read's Rule also provide insight into how soil factors structure

331   the fine-scale distributions of tree symbioses within our grid cells. For example, while at a coarse

332   scale we find that EM trees are relatively rare in many wet tropical forests, individual tropical

333   sites in our raw data span the full range from 0 – 100 % EM basal area. In much of the wet

334   tropics, these EM dominated sites exist as outliers within a matrix of predominantly AM trees. In

335   an apparent exception that proves Read's Rule, in aseasonal warm neotropical climates, which

16

336   accelerate leaf-decomposition and promote regional AM dominance (Figure 3), EM dominated

337   tree stands can develop in sites where poor soils and recalcitrant litter slow decomposition and N

338   mineralization[26,51]. Landscape-scale variation in the relative abundance of symbiotic states also

339   changes along climate gradients, with variability highest in xeric and temperate biomes (Figure

340   S2), suggesting that the potential of local nutrient variability to favor particular symbioses is

341   contingent on climate.

342   Whereas EM trees are associated with ecosystems where plant growth is thought to be

343   primarily N-limited, N-fixer trees are not. Our results highlight the global extent of the "N-

344   cycling paradox," wherein some metrics suggest that N-limitation is greater in the temperate

345   zone[46-48], yet N-fixing trees are relatively more common in the tropics[20,52,53] (Figure 3A). We

346   find that N-fixers, which we estimate represent 7% of all trees, dominate forests with annual max

347   temperatures >35°C and alkaline soils (particularly in North America and Africa, Figure 2C).

348   They have the highest relative abundance in xeric shrublands (24%), tropical savannas (21%),

349   and dry broadleaf forest biomes (20%), but are nearly absent from boreal forests (<1%) (Figure

350   3A, Figure 4). The decline in N-fixer tree abundance we observed with increasing latitude is also

351   associated with a previously documented latitudinal shift in the identity of N-fixing microbes,

352   from facultative N-fixing rhizobial bacteria in tropical forests to obligate N-fixing actinorhizal

353   bacteria in temperate forests[52]. Our data are not capable of fully disentangling the several

354   hypotheses that have been proposed to reconcile the N-cycling paradox[20,54]. However, our results

355   are consistent with the model prediction[22] and regional empirical evidence[27,55,56] that N-fixing

356   trees are particularly important in arid biomes. Based primarily on the observed positive,

357   nonlinear association of N-fixer relative abundance with the mean temperature of the hottest

358 month (Figure 2C), our models predict a two-fold increase in N-fixer relative abundance when

359 transitioning from humid to dry tropical forest biomes (Figure 3A).

360   Although soil microbes are a dominant component of forests, both in terms of diversity

361 and ecosystem functioning[5,6,11], identifying global-scale microbial biogeographic patterns

362 remains an ongoing research priority. Our analyses confirm that Read's Rule, which is one of the

363 first proposed biogeographic rules specific to microbial symbioses, successfully describes global

364 transitions between mycorrhizal guilds. More generally, climate driven turnover among the

365 major plant-microbe symbioses represents a fundamental biological pattern in the Earth system,

366 as forests transition from low-latitude arbuscular mycorrhizal, to N-fixer, to high-latitude

367 ectomycorrhizal ecosystems. The predictions of our model (which we make available as a global

368 raster layer) can now be used to represent these critical ecosystem variations in global

369 biogeochemical models used to predict climate-biogeochemical feedbacks within and between

370 trees, soils, and the atmosphere. Additionally, the layer containing the proportion abundance of

371 N-fixing trees can be used to map potential symbiotic N-fixation, which links together

372 atmospheric pools of C and N. Future work can extend our findings to incorporate multiple plant

373 growth forms and non-forested biomes, where similar patterns likely exist, to generate a

374 complete global perspective. Our predictive maps leverage the most comprehensive global forest

375 dataset to generate the first quantitative global map of forest tree symbioses, demonstrating how

376 nutritional mutualisms are coupled with the global distribution of plant communities.

496   Ivory Coast; the Queensland Herbarium and past Queensland Government Forestry and Natural

497   Resource Management Departments and staff for data collection for over seven decades. Ziaur

498   Rahman Laskar, Salam Dilip, Bijit, Bironjoy and Samar; Badru Mugerwa and Emmanuel

499   Akampurira, together with a team of field assistants (Valentine and Lawrence); all persons who

500   made the Third Spanish Forest Inventory possible, especially the main coordinator, J. A.

501   Villanueva (IFN3); Italian and Friuli Venezia Giulia Forest Services (Italy); Rafael Ávila and

502   Sharon van Tuylen, Insituto Nacional de Bosques (INAB), Guatemala for facilitating

503   Guatemalan data; The National Focal Center for Forest condition monitoring of Serbia (NFC),

504   Institute of Forestry, Belgrade, Serbia; The Thünen Institute of Forest Ecosystems (Germany) for

505   providing National Forest Inventory data; All TEAM data provided by the Tropical Ecology

506   Assessment and Monitoring (TEAM) Network, a collaboration between Conservation

507   International, the Missouri Botanical Garden, the Smithsonian Institution, and the Wildlife

508   Conservation Society, and partially funded by these institutions, the Gordon and Betty Moore

509   Foundation, and other donors, with thanks to all current and previous TEAM site manager and

510   other collaborators that helped collecting data; The people of the Redi Doti, Pierrekondre and

511   Cassipora village who were instrumental in assisting with the collection of data and sharing local

512   knowledge of their forest; and the dedicated members of the field crew of Kabo 2012 census.

References

516   1   Batterman, S. A. et al. Key role of symbiotic dinitrogen fixation in tropical forest
517   secondary succession. Nature **502**, 224-227, doi:10.1038/nature12525 (2013).
518   2   Shah, F. et al. Ectomycorrhizal fungi decompose soil organic matter using oxidative
519   mechanisms adapted from saprotrophic ancestors. New Phytol **209**, 1705-1719,
520   doi:10.1111/nph.13722 (2016).

521   3   Averill, C., Turner, B. L. & Finzi, A. C. Mycorrhiza-mediated competition between
522   plants and decomposers drives soil carbon storage. Nature **505**, 543-+,
523   doi:10.1038/nature12901 (2014).
524   4   Clemmensen, K. E. et al. Roots and associated fungi drive long-term carbon
525   sequestration in boreal forest. Science **339**, 1615-1618, doi:10.1126/science.1231923
526   (2013).
527   5   Cheeke, T. E. et al. Dominant mycorrhizal association of trees alters carbon and nutrient
528   cycling by selecting for microbial groups with distinct enzyme function. New Phytol.
529   **214**, 432-442, doi:10.1111/nph.14343 (2017).
530   6   Terrer, C., Vicca, S., Hungate, B. A., Phillips, R. P. & Prentice, I. C. Mycorrhizal
531   association as a primary control of the CO2 fertilization effect. Science **353**, 72-74,
532   doi:10.1126/science.aaf4610 (2016).
533   7   Johnson, D. J., Beaulieu, W. T., Bever, J. D. & Clay, K. Conspecific negative density
534   dependence and forest diversity. Science **336**, 904‚Äì907 (2012).
535   8   Brundrett, M. C. in Biogeography of Mycorrhizal Symbiosis   533-556 (Springer, 2017).
536   9   Averill, C. & Hawkes, C. V. Ectomycorrhizal fungi slow soil carbon cycling. Ecol Lett
537   **19**, 937-947, doi:10.1111/ele.12631 (2016).
538   10   Bennett, J. A. et al. Plant-soil feedbacks and mycorrhizal type influence temperate forest
539   population dynamics. Science **355**, 181-184 (2017).
540   11   Phillips, R. P., Brzostek, E. & Midgley, M. G. The mycorrhizal-associated nutrient
541   economy: a new framework for predicting carbon-nutrient couplings in temperate forests.
542   New Phytol. **199**, 41-51, doi:10.1111/nph.12221 (2013).
543   12   Oleson, K. W. et al. Technical description of version 4.0 of the Community Land Model
544   (CLM). (2010).
545   13   Crowther, T. W. et al. Mapping tree density at a global scale. Nature **525**, 201 (2015).
546   14   Heijden, M. G., Martin, F. M., Selosse, M. A. & Sanders, I. R. Mycorrhizal ecology and
547   evolution: the past, the present, and the future. New Phytol. **205**, 1406-1423 (2015).
548   15   Lindahl, B. D. & Tunlid, A. Ectomycorrhizal fungi–potential organic matter
549   decomposers, yet not saprotrophs. New Phytol. **205**, 1443-1447 (2015).
550   16   Liu, X. et al. Partitioning of soil phosphorus among arbuscular and ectomycorrhizal trees
551   in tropical and subtropical forests. Ecol Lett **21**, 713-723 (2018).
552   17   Zhu, K., McCormack, M. L., Lankau, R. A., Egan, J. F. & Wurzburger, N. Association of
553   ectomycorrhizal trees with high carbon-to-nitrogen ratio soils across temperate forests is
554   driven by smaller nitrogen not larger carbon stocks. Journal of Ecology **106**, 524-535
555   (2018).
556   18   Binkley, D., Sollins, P., Bell, R., Sachs, D. & Myrold, D. Biogeochemistry of adjacent
557   conifer and alder-conifer stands. Ecology **73**, 2022-2033 (1992).
558   19   Leake, J. et al. Networks of power and influence: the role of mycorrhizal mycelium in
559   controlling plant communities and agroecosystem functioning. Canadian Journal of
560   Botany **82**, 1016-1045 (2004).
561   20   Hedin, L. O., Brookshire, E. N. J., Menge, D. N. L. & Barron, A. R. in Annual Review of
562   Ecology Evolution and Systematics Vol. 40 Annual Review of Ecology Evolution and
563   Systematics   613-635 (Annual Reviews, 2009).
564   21   Read, D. J. Mycorrhizas in Ecosystems. Experientia **47**, 376-391, doi:Doi
565   10.1007/Bf01972080 (1991).

566 22 Houlton, B. Z., Wang, Y.-P., Vitousek, P. M. & Field, C. B. A unifying framework for
567   dinitrogen fixation in the terrestrial biosphere. Nature **454**, 327 (2008).
568 23 Bueno, C. G. et al. Plant mycorrhizal status, but not type, shifts with latitude and
569   elevation in Europe. Global Ecology and Biogeography **26**, 690-699 (2017).
570 24 Soudzilovskaia, N. A., Vaessen, S., van't Zelfde, M. & Raes, N. in Biogeography of
571   Mycorrhizal Symbiosis   223-235 (Springer, 2017).
572 25 Brundrett, M. C. & Tedersoo, L. Evolutionary history of mycorrhizal symbioses and
573   global host plant diversity. New Phytol. (2018).
574 26 Peay, K. G. The mutualistic niche: mycorrhizal symbiosis and community dynamics.
575   Annual Review of Ecology, Evolution, and Systematics **47**, 143-164 (2016).
576 27 Pellegrini, A. F., Staver, A. C., Hedin, L. O., Charles-Dominique, T. & Tourgee, A.
577   Aridity, not fire, favors nitrogen-fixing plants across tropical savanna and forest biomes.
578   Ecology **97**, 2177-2183 (2016).
579 28 Liang, J. et al. Positive biodiversity-productivity relationship predominant in global
580   forests. Science **354**, aaf8957 (2016).
581 29 Brundrett, M. C. Mycorrhizal associations and other means of nutrition of vascular
582   plants: understanding the global diversity of host plants by resolving conflicting
583   information and developing reliable means of diagnosis. Plant and Soil **320**, 37-77,
584   doi:10.1007/s11104-008-9877-9 (2009).
585 30 Werner, G. D., Cornwell, W. K., Cornelissen, J. H. & Kiers, E. T. Evolutionary signals of
586   symbiotic persistence in the legume–rhizobia mutualism. Proceedings of the National
587   Academy of Sciences **112**, 10262-10269 (2015).
588 31 Afkhami, M. E. et al. Symbioses with nitrogen-fixing bacteria: nodulation and
589   phylogenetic data across legume genera. Ecology **99**, 502-502 (2018).
590 32 Tedersoo, L. et al. Global database of plants with root-symbiotic nitrogen fixation: Nod
591   DB. Journal of Vegetation Science (2018).
592 33 Wang, B. & Qiu, Y.-L. Phylogenetic distribution and evolution of mycorrhizas in land
593   plants. Mycorrhiza **16**, 299-363 (2006).
594 34 McGuire, K. et al. Dual mycorrhizal colonization of forest-dominating tropical trees and
595   the mycorrhizal status of non-dominant tree and liana species. Mycorrhiza **18**, 217-222
596   (2008).
597 35 Palosuo, T., Liski, J., Trofymow, J. & Titus, B. Litter decomposition affected by climate
598   and litter quality—testing the Yasso model with litterbag data from the Canadian intersite
599   decomposition experiment. Ecological Modelling **189**, 183-198 (2005).
600 36 Tuomi, M. et al. Leaf litter decomposition—estimates of global variability based on
601   Yasso07 model. Ecological Modelling **220**, 3362-3371 (2009).
602 37 Bradford, M. A. et al. Climate fails to predict wood decomposition at regional scales.
603   Nature Climate Change **4**, 625 (2014).
604 38 Ma, Z. et al. Evolutionary history resolves global organization of root functional traits.
605   Nature (2018).
606 39 Staver, A. C., Archibald, S. & Levin, S. Tree cover in sub-Saharan Africa: rainfall and
607   fire constrain forest and savanna as alternative stable states. Ecology **92**, 1063-1072
608   (2011).
609 40 Scheffer, M., Carpenter, S., Foley, J. A., Folke, C. & Walker, B. Catastrophic shifts in
610   ecosystems. Nature **413**, 591 (2001).

611   41   Parmesan, C. & Yohe, G. A globally coherent fingerprint of climate change impacts
612   across natural systems. Nature **421**, 37 (2003).
613   42   Reich, P. B. & Oleksyn, J. Climate warming will reduce growth and survival of Scots
614   pine except in the far north. Ecol Lett **11**, 588-597, doi:10.1111/j.1461-
615   0248.2008.01172.x (2008).
616   43   Fernandez, C. W. & Kennedy, P. G. Revisiting the 'Gadgil effect': do interguild fungal
617   interactions control carbon cycling in forest soils? New Phytol. **209**, 1382-1394,
618   doi:10.1111/nph.13648 (2016).
619   44   Reich, P. B. et al. Geographic range predicts photosynthetic and growth response to
620   warming in co-occurring tree species. Nature Climate Change **5**, 148 (2015).
621   45   Hanewinkel, M. & Peyron, J.-L. Tackling climate change—the contribution of scientific
622   knowledge in forestry. Ann Forest Sci **71**, 113-115 (2014).
623   46   Vitousek, P. M. Litterfall, nutrient cycling, and nutrient limitation in tropical forests.
624   Ecology **65**, 285-298 (1984).
625   47   McGroddy, M. E., Daufresne, T. & Hedin, L. O. Scaling of C: N: P stoichiometry in
626   forests worldwide: Implications of terrestrial redfield-type ratios. Ecology **85**, 2390-2401
627   (2004).
628   48   Reich, P. B. & Oleksyn, J. Global patterns of plant leaf N and P in relation to temperature
629   and latitude. Proceedings of the National Academy of Sciences of the United States of
630   America **101**, 11001-11006 (2004).
631   49   Vitousek, P. M. & Sanford Jr, R. L. Nutrient cycling in moist tropical forest. Annu Rev
632   Ecol Syst **17**, 137-167 (1986).
633   50   Grunwald, S., Thompson, J. & Boettinger, J. Digital soil mapping and modeling at
634   continental scales: Finding solutions for global issues. Soil Science Society of America
635   Journal **75**, 1201-1213 (2011).
636   51   Corrales, A., Mangan, S. A., Turner, B. L. & Dalling, J. W. An ectomycorrhizal nitrogen
637   economy facilitates monodominance in a neotropical forest. Ecol Lett **19**, 383-392,
638   doi:10.1111/ele.12570 (2016).
639   52   Menge, D. N., Lichstein, J. W. & Ángeles-Pérez, G. Nitrogen fixation strategies can
640   explain the latitudinal shift in nitrogen-fixing tree abundance. Ecology **95**, 2236-2245
641   (2014).
642   53   Ter Steege, H. et al. Continental-scale patterns of canopy tree composition and function
643   across Amazonia. Nature **443**, 444 (2006).
644   54   Menge, D. N. et al. Why are nitrogen-fixing trees rare at higher compared to lower
645   latitudes? Ecology **98**, 3127-3140 (2017).
646   55   Liao, W., Menge, D. N., Lichstein, J. W. & Ángeles-Pérez, G. Global climate change will
647   increase the abundance of symbiotic nitrogen-fixing trees in much of North America.
648   Global Change Biol (2017).
649   56   Gei, M. et al. Legume abundance along successional and rainfall gradients in Neotropical
650   forests. Nature ecology & evolution, 1 (2018).
651